



## UvA-DARE (Digital Academic Repository)

### Radiative stabilization of the doubly-excited 4l4l' and 4l5l' singlet terms in Ne8+

van der Hart, H.W.; Vaeck, N.; Hansen, J.E.

**DOI**

[10.1088/0953-4075/28/24/007](https://doi.org/10.1088/0953-4075/28/24/007)

**Publication date**

1995

**Published in**

Journal of Physics. B, Atomic, Molecular and Optical Physics

[Link to publication](#)

**Citation for published version (APA):**

van der Hart, H. W., Vaeck, N., & Hansen, J. E. (1995). Radiative stabilization of the doubly-excited 4l4l' and 4l5l' singlet terms in Ne8+. *Journal of Physics. B, Atomic, Molecular and Optical Physics*, 28, 5207-5228. <https://doi.org/10.1088/0953-4075/28/24/007>

**General rights**

It is not permitted to download or to forward/distribute the text or part of it without the consent of the author(s) and/or copyright holder(s), other than for strictly personal, individual use, unless the work is under an open content license (like Creative Commons).

**Disclaimer/Complaints regulations**

If you believe that digital publication of certain material infringes any of your rights or (privacy) interests, please let the Library know, stating your reasons. In case of a legitimate complaint, the Library will make the material inaccessible and/or remove it from the website. Please Ask the Library: <https://uba.uva.nl/en/contact>, or a letter to: Library of the University of Amsterdam, Secretariat, Singel 425, 1012 WP Amsterdam, The Netherlands. You will be contacted as soon as possible.

# Radiative stabilization of the doubly-excited $4l4l'$ and $4l5l'$ singlet terms in $\text{Ne}^{8+}$

Hugo W van der Hart†, Nathalie Vaeck†§ and Jørgen E Hansen

Van der Waals–Zeeman Institute, University of Amsterdam, Valckenierstraat 65,  
NL-1018 XE Amsterdam, The Netherlands

Received 19 May 1995, in final form 4 August 1995

**Abstract.** Calculations concerning the competition between radiative and non-radiative decay for doubly-excited  $4lnl'$  ( $n = 4, 5$ ) singlet states in  $\text{Ne}^{8+}$  are reported. Recent coincidence experiments have been interpreted as showing that for the  $4l4l'$  states in  $\text{Ne}^{8+}$ , as well as in the isoelectronic  $\text{N}^{5+}$  and  $\text{O}^{6+}$  systems, radiation contributes more than 50% to the total decay. The  $4l4l'$  states in  $\text{Ne}^{8+}$  are, as in  $\text{N}^{5+}$  and  $\text{O}^{6+}$ , degenerate with the  $3lnl'$  Rydberg states and a considerable mixing exists between the two, which leads to an increase in the radiative decay probability. In the free  $\text{Ne}^{8+}$  ion we find that radiative decay accounts for 29% of the total decay for the singlet terms assuming a statistical population distribution. The results vary considerably between terms and the total radiative yield is strongly dependent on the initial population distribution. The branching ratio is similar to the ratio obtained under similar conditions for  $\text{O}^{6+}$ . The similarity is ascribed to two competing effects: the lowering of the  $4l4l'$  states relative to the  $3lnl'$  series with increasing  $Z$ , which favours decay through autoionization, and the  $Z^4$  behaviour of the radiative decay rates, which has the opposite effect. The free ion results are compared to results including the auto-transfer to Rydberg states (ATR) mechanism. In  $\text{N}^{5+}$  we have shown that this effect leads to an appreciable reduction in the radiative yield. For  $\text{Ne}^{8+}$ , the ATR mechanism is less important but we conclude that also here the effect on average is a (small) reduction in radiative yield. This is because the ATR mechanism is usually so effective that the  $4l4l'$  population is transferred to low Rydberg states. These autoionize in light ions while they have a larger probability for radiative decay with increasing  $Z$ . This seems to account for a large part of the difference between the ATR results in  $\text{N}^{5+}$  and  $\text{Ne}^{8+}$ . We report the results of an alternative approach in which part of the collision dynamics is included and we find that the ATR model is rather sensitive to a number of parameters, which at the moment are not known very well. For the  $4l5l'$  states, which are located above the  $N = 3$  threshold, radiative decay accounts for 6% of the total decay, much less than for the  $4l4l'$  states, due to the opening of autoionization channels to the  $N = 3$  thresholds for the  $4l5l'$  states. Assuming a statistical population distribution, the theoretical results are in clear disagreement with recent observations for both  $4l4l'$  and  $4l5l'$  manifolds. However, we conclude that it is necessary to obtain a more definite idea about the real population distribution before it is possible to make meaningful comparisons with the observed radiative yields.

## 1. Introduction

The competition between radiative and non-radiative decay of doubly-excited states in few-electron systems has attracted much interest in the last couple of years. The reason is

† Present address: Department of Applied Mathematics and Theoretical Physics, The Queen's University of Belfast, Belfast BT7 1NN, Northern Ireland.

‡ Senior Research Assistant of the Belgian National Fund for Scientific Research (FNRS).

§ Present address: Laboratoire de Chimie Physique Moléculaire, Université Libre de Bruxelles, CP160/09, 50 av. F-D Roosevelt, B-1050 Bruxelles, Belgium.

the recent observation of a large probability for true double capture (TDC), in which both electrons are retained on the projectile, in ion-atom collisions. In double-electron capture by a highly-charged projectile from a neutral gas target the transferred electrons are captured predominantly in excited states of the projectile. Earlier it was expected that such states would preferentially autoionize and thus lead to a single electron remaining on the projectile. The recent observations (Stolterfoht *et al* 1990, Roncin *et al* 1991) of large TDC probabilities in certain collisions has, therefore, stimulated much interest in such processes. In the following we usually call the branching ratio for radiative decay the '(radiative) stabilization ratio', since this process leads to TDC. The ratio obtained for all singlet terms assuming a particular population distribution, usually statistical, is called the 'overall' stabilization ratio.

If the electrons are captured one at a time in a two-step process, the extended classical over the barrier model (ECBM) (Bárány *et al* 1985, Niehaus 1986) predicts that both electrons have more or less equal  $n$  values and it has been shown, for example for  $C^{4+}$ , that, theoretically, radiative decay accounts for 2% of the total decay for  $2l2l'$  states and as little as 0.3% for  $3l3l'$  states (van der Hart and Hansen 1993). Similar values are expected for neighbouring ions. Only in the case of the capture process populating  $2pnl$  states with  $n$  in the range 6–12 was radiative decay found to contribute significantly to the total decay (Stolterfoht *et al* 1990, Chen and Lin 1991, van der Hart and Hansen 1993), thus seriously affecting the ejected-electron yields. However, recently high degrees of radiative decay, > 50%, have been reported for doubly-excited  $nl n'l'$  states with  $n \approx n'$  (Roncin *et al* 1991, 1993b, Gaboriaud *et al* 1993, Martin *et al* 1994). For instance, a stabilization ratio of 25% was measured for collisions of  $O^{8+}$  on Ar (Gaboriaud *et al* 1993). In this experiment, 75% of the total population was assigned to  $4l5l'$  states and 25% to the  $4l4l'$  complex, leading to a stabilization ratio of 59% for the latter. Similar amounts of radiative stabilization have now been reported for a variety of collision schemes (Roncin *et al* 1991, 1993b, Gaboriaud *et al* 1993) and recently Roncin *et al* (1993b) have obtained similar values for  $Ne^{10+}$  on Ne.

Whereas much theoretical work has been reported concerning doubly-excited states in highly-charged ions below the  $N = 2$  and  $N = 3$  thresholds, the  $4lnl'$  states have been studied to a much lesser extent and the first complete study was reported only recently (van der Hart *et al* 1994). In two-electron systems, the  $4l4l'$  states are the lowest states that can overlap a Rydberg series, namely the  $3lnl'$  series. Ho (1980) has determined the energies of the  $4l4l'$   $^1S^e$ ,  $^1P^o$  and  $^3P^o$  terms for  $Z$  up to 10 and found that for low  $Z$ , the electron repulsion moves these  $4l4l'$  terms above threshold, whereas for  $Ne^{8+}$  only one of them lies above the  $N = 3$  threshold. In these complex-coordinate calculations, the non-radiative decay rates of the  $4l4l'$  states were also determined, but Bachau *et al* (1993) have pointed out that the calculated rates appear to consist of autoionization rates towards  $2lel'$  continua plus a transfer rate to  $3lnl'$  states. Configuration interaction methods with hydrogenic basis sets have also been applied to the calculation of autoionization in  $Ne^{8+}$ . Bachau (1984) was the first to use such a basis with  $4 \leq n \leq 7$ , while Chetioui *et al* (1990) extended the calculations. Bachau (1993) and Sánchez and Bachau (1995) have reported radiative rates for  $^1D^o$  terms in the free atom. Figure 1 shows the position of the  $4l4l'$  singlet terms in  $Ne^{8+}$  relative to the Rydberg series.

The purpose of this paper is twofold. The first is to provide a complete set of data for the singlet terms in the free  $Ne^{8+}$  ion including both radiative and autoionization decay probabilities. The second is to study the  $Z$  dependence of the decay rates and, in particular, of the branching ratio for radiative decay. Under the assumption of a statistical population distribution over the  $4l4l'$  complex, the overall stabilization ratio obtained for the free  $O^{6+}$  ion is about a factor of two smaller than observed. To explain this type of discrepancy,

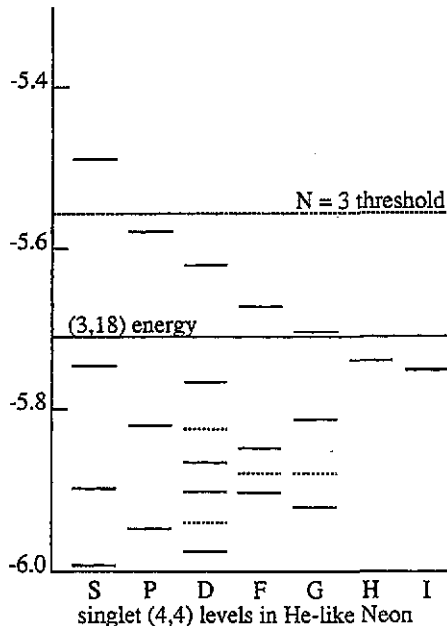


Figure 1. The positions of the singlet  $4l4l'$  terms in the free  $Ne^{8+}$  ion relative to the  $3lnl'$  series and the  $N = 3$  thresholds. Broken lines are used to represent terms of the unnatural parity ( $\pi = (-1)^{L+1}$ ) while the natural parity terms ( $\pi = (-1)^L$ ) are represented by full lines. The average  $3l18l'$  energy is also indicated. The interaction with the  $3lnl'$  Rydberg series is not included in the calculation of the energies.

Bachau *et al* (1992) proposed the auto-transfer to Rydberg states (ATR) mechanism, in which the  $4l4l'$  levels are shifted to lower energies during the collision due to a type of post-collision interaction (PCI) effect, and on the way out of the collision those states that lie above or close to threshold in the free atom can lose their  $4l4l'$  character through crossings with the  $3lnl'$  levels. Roncin *et al* (1993a) carried out two types of time-dependent close-coupling calculations of the effect of the ATR mechanism for the  $N^{5+}$  ion. One in which the  $4l4l'$  energies were fixed at the free-atom values, called static close-coupling, and another in which the  $4l4l'$  energies varied with respect to the  $N = 3$  threshold in a model calculation called dynamic close coupling. In the former calculation, an overall stabilization ratio of 15% was observed, which increased to 18% when the ATR effect was included, assuming a statistical population distribution. Under the latter assumption, the difference with the interpretation of the experimental results for this ion, > 52% (Gaboriaud *et al* 1993), remained large. For the free  $N^{5+}$  atom we obtained (van der Hart and Hansen 1994) a theoretical stabilization ratio larger than the ATR value, which allowed us to conclude that the ATR mechanism in the close-coupling formulation employed by Roncin *et al* (1993a) is 'too effective' and transfers population primarily into low Rydberg states that autoionize. The disagreement with the static close-coupling calculation by Roncin *et al* (1993a), which gave a smaller value than obtained in our free-atom calculation, was ascribed primarily to the neglect of interference between the autoionization rates for the  $4l4l'$  and  $3lnl'$  components, which was found to be important for the free atom. Recently Roncin *et al* (1993b) have predicted a much larger stabilization ratio, 40%, for the singlet terms in  $Ne^{8+}$  within the same ATR model, and one reason for the present study of the isoelectronic behaviour of the stabilization ratios in the free atom is to shed light on the reasons for this difference

between  $O^{6+}$  and  $Ne^{8+}$ .

The large stabilization ratio obtained by Roncin *et al.* (1993b) for  $Ne^{8+}$  is at first sight surprising. The original ATR model (Bachau *et al.* 1992) assumed that large degrees of stabilization are obtained only for those ions in which the  $4l4l'$  states cross the  $N = 3$  threshold on the way out of the collision and there is only one such state in  $Ne^{8+}$ . However, it was soon realized (Vaeck and Hansen 1993, Roncin *et al.* 1993a) that also states high enough in the Rydberg series can be influenced. With increasing  $Z$  two competing effects can be distinguished. One is the lowering of the  $4l4l'$  states relative to  $3lnl'$ , which leads to overlap with lower members of the Rydberg series and thus a reduction in the presumed effectiveness of the ATR mechanism. The other is the  $Z^4$  dependence of the radiative decay rates which, in conjunction with the weak  $Z$  dependence of the non-radiative rates, will lead to radiative decay becoming the dominant decay mode for lower and lower members of the Rydberg series. The ATR results due to Roncin *et al.* (1993b) indicate that the latter is the more important effect and this is confirmed here by calculations which include some aspects of the ATR mechanism. The clue to the understanding of why this is so lies in the observation that the mechanism is so effective that primarily low Rydberg states are populated and in general very little  $4l4l'$  population is transferred to the high Rydberg states (van der Hart and Hansen 1994). This means that the mechanism becomes effective with regard to stabilization only for ions where radiative decay is dominant for *low* Rydberg states, thus for  $Ne^{8+}$  instead of  $N^{5+}$ . With a further increase of  $Z$ , however, the  $4l4l'$  states will soon lie so low that the mechanism does lose its effectiveness. The implication is that the ATR mechanism on average must lead to a reduction in the radiative decay rate and consequently a *reduction* in stabilization (van der Hart and Hansen 1994) which makes it particularly interesting to understand the reason for the large *increase* in stabilization reported by Roncin *et al.* (1993b) for  $Ne^{8+}$ .

However, there are other aspects to the stabilization of the  $4l4l'$  states. Since the stabilization ratio is strongly term dependent, the problem of stabilization cannot be separated from the question of which states are populated within the manifold. The first question, which must be addressed, is how the  $4l4l'$  states are populated. The ECBM, based on the independent particle model, has been used successfully to predict cross sections and principal quantum numbers for the multiply-excited states created in charge transfer processes (Niehaus 1986). In the case of a collision of an  $O^{8+}$  ion with Ar, the model predicts capture into  $4l5l'$  states, as indeed is observed experimentally (Gaboriaud *et al.* 1993), while the  $4l4l'$  states lie outside the reaction window. Thus other population mechanisms probably also contribute. The production of Rydberg states in ion-atom collisions has been noticed earlier (Stolterfoht *et al.* 1986, Stolterfoht 1993). If there is a direct population of  $3lnl'$  states this would give rise to a high degree of stabilization (Vaeck *et al.* 1993a, b) and it is difficult from the electron spectra to discriminate between the  $3lnl'$  states and the overlapping  $4l4l'$  states. A number of recent experiments have found large populations of  $3lnl'$  states outside the region of overlap with  $4l4l'$  (de Nijs *et al.* 1994, Frémont *et al.* 1994, Bordenave-Montesquieu *et al.* 1994). This lies behind the present interest in the production mechanism associated with double capture. So far most studies have considered only parts of the observed spectra and a theory that can explain the population of the whole spectrum is still missing.

On the other hand, populating Rydberg states is no panacea. Only if the  $n$  value of the outer electron is large enough is radiative decay ensured (Vaeck *et al.* 1993a, b) and what 'large enough' means depends on  $Z$ . Thus the problem is very complex, which explains the large amount of work that has been reported recently.

In this paper, we consider the properties of the singlet  $4l4l'$  states in the free  $Ne^{8+}$

ion, taking the interaction with the Rydberg series into account, and compare with the stabilization ratios obtained via the ATR approach and with the ratios obtained for  $O^{6+}$ . In order to understand the differences between the ATR results and the free-atom values for  $Ne^{8+}$  and  $O^{6+}$ , we report also a semi-static calculation, which includes some of the features of the dynamic calculation. In addition, the  $4l5l'$  states are considered, since also for these states there is disagreement between the experimental and theoretical stabilization ratios in  $O^{6+}$  under the assumption of a statistical population distribution. After this work was finished Sánchez and Bachau (1995) and Bachau and Sánchez (1995) published ATR calculations for the  $4l4l'$  states in  $Ne^{8+}$  that support the conclusions drawn here.

## 2. Theoretical approach

The calculational method applied to  $O^{6+}$  has already been described in some detail by van der Hart *et al* (1994), so we give only a brief description here. The main problem in the calculation is how to accurately describe the Rydberg states and their interactions. Because of the  $n^2$  scaling of the mean radius of a Rydberg state, it is necessary to span a large radial distance. Using  $B$ -splines, it is possible to get an accurate representation of the 'low' ( $n < 40$ ) Rydberg states in  $Ne^{8+}$  using a cavity with a radius of 400 au. Figure 1 shows that those  $4l4l'$  singlet terms which lie below the  $N = 3$  threshold lie in the region up to  $n \approx 25$ , except the highest  $^1P^o$  state discussed later.

We have used three different one-electron  $B$ -spline based basis sets in this calculation. The first one consists of 25  $B$ -spline solutions to the one-electron Schrödinger equation for  $Ne^{9+}$  with angular momentum up to  $l = 8$ . This set is used in the determination of energies and wavefunctions for the  $4lnl'$  states in the absence of the interaction with the  $3lnl'$  series. Since we are interested in low-lying bound states, the knot points of the  $B$ -spline set of order seven are distributed exponentially within a small cavity of radius 32 au. The second basis set describes the  $nl$  Rydberg electrons. It consists of 141  $B$ -splines of order nine defined in the 400 au box, mentioned above, using an exponential knot set. The third and last  $B$ -spline set of order seven is used to generate pseudo-continuum wavefunctions in the small box. In order to represent the oscillatory behaviour of continuum wavefunctions, 22 knot points are distributed exponentially up to  $r = 0.48$  au and 116 distributed linearly from 0.48 au up to 32 au. Whereas the  $R^0(3lnl', 3lnl')$  matrix elements, which describe the interaction within the Rydberg series, require an integration over the large box used for the second set, for continuum states a small box is sufficient since the  $R^k$  interaction matrix elements involved in the autoionization process contain  $1s$ ,  $2l$  or  $3l$  wavefunctions that go to zero well before 32 au, thus forcing the contribution to the interaction matrix element to zero outside the small box.

We have used the truncated diagonalization method (TDM), in which all contributions from  $1sn/\epsilon l$ ,  $2ln/\epsilon l'$  and  $3ln/\epsilon l'$  are neglected, to determine energies and eigenfunctions of the  $4lnl'$  states. Using the expansions described earlier (van der Hart *et al* 1994), this results in matrix sizes between 800 and 2600. Since only the lowest eigenfunctions and eigenvalues are of interest, we use a modified Davidson algorithm (Davidson 1975) to determine only the lowest 15 solutions for each  $LS$  symmetry. In this basis, the eigenstates representing the  $4l4l'$  states will be called the 'preliminary'  $4l4l'$  terms.

Subsequently, we determine the interaction between the  $3lnl'$  states and the 'preliminary'  $4l4l'$  states in a second configuration interaction (CI) calculation. There is a maximum of six  $3lnl'$  Rydberg series for any symmetry, and by 'freezing' the 'preliminary'  $4l4l'$  eigenvectors it is possible to keep the matrix size of this CI calculation down to less than 850. This is important since the matrices involved in this step of the calculation must be

fully diagonalized, because a complete description of the lower part of the Rydberg series is required. The Rydberg series are listed in van der Hart *et al* (1994) for each symmetry (we note that there is a misprint in table 2 of that paper where  $1P^o$  should be  $1P^e$ ). The highest  $1P^o$  state lies close to the  $N = 3$  threshold and we have therefore extended the cavity involved in the determination of the Rydberg states to 800 au in order to describe accurately Rydberg states with  $n$  up to 50 for this symmetry. The number of  $B$ -splines is also increased to 191 splines, which in the second step leads to a matrix of size 953.

The lifetime of the mixed  $4l4l'$  and  $3lnl'$  states with respect to autoionization towards all available continua (the decay to the  $N = 2$  limits being the most important) is determined using Fermi's golden rule (Merzbacher 1961). For the  $4l5l'$  states only autoionization towards the nearest  $N = 3$  limits is calculated, since this is expected to be the dominant autoionization channel for these states. In all calculations, the coupling between degenerate continua is not included, since we are only interested in total rates, for which the coupling has been shown to have a negligible effect in ionized systems (Martín *et al* 1991).

The radiative rates for the  $4l4l'$  and  $4l5l'$  states are determined as follows. Using the basis set for the preliminary  $4lnl'$  states, we have determined the 15 lowest  $1snl$ ,  $2lnl'$ , and  $3lnl'$  states for all symmetries present in the  $4l4l'$  and  $4l5l'$  complexes. The radiative rates are then determined by summing all possible radiative decays to these lower states. For all symmetries, the states with  $n = 5$  are among the lowest 15 states, so all important one-electron transitions are taken into account. With this cut-off also some transitions to continuum  $1seI$  states are included in the radiative decay, but it was checked that their contribution is negligible. A few radiative decay paths are not taken into account, such as decay from  $1K^o$  to  $1K^e$ , but, on the other hand, this corresponds in the present study to a two-electron transition from an  $fg$  state to a  $di$  state and the associated transition rate is expected to be negligible.

The average radiative decay rates for the unperturbed  $3lnl'$  Rydberg states,  $A_{\text{Ryd}}^r$ , are obtained for each  $LS$  symmetry from data for  $O^{6+}$  (van der Hart *et al* 1994) scaled with  $Z^4$ . Since this decay mode is dominated by radiative decay of the inner electron (Vaeck *et al* 1993a), the decay rate is assumed to be independent of  $n$ . Finally, the radiative decay rate of a mixed  $4l4l' + 3lnl'$  state is given by

$$A^r = A_{\text{Ryd}}^r + \sum_{N=1}^{N_{44}} C_N^2 (A_N^r - A_{\text{Ryd}}^r) \quad (1)$$

with  $N_{44}$  the number of  $4l4l'$  states within the particular symmetry, while  $C_N$  and  $A_N^r$  are the expansion coefficient and the radiative decay rate, respectively, for the  $N$ th  $4l4l'$  state. No interference between radiative decay from the  $4l4l'$  part of the eigenvector and decay from the  $3lnl'$  part is taken into account, but since the final states, which are important, differ for the  $4l4l'$  and  $3lnl'$  basis states, this effect is expected to be small. Interference between decay from different  $4l4l'$  basis states is included in the absence of the interaction with the  $3lnl'$  states and, since the mixing between the preliminary  $4l4l'$  states introduced by the interaction with  $3lnl'$  is small, these values are expected to be quite accurate. We note that this approach contains fewer approximations than that used for  $O^{6+}$  (van der Hart *et al* 1994).

The branching ratio for radiative decay is defined for each individual state by

$$R^r = \frac{A^r}{A^a + A^r} \quad (2)$$

with  $A^a$  and  $A^r$  the total autoionization rate and total radiative decay rate, respectively. For the  $4l5l'$  configurations, this value is reported for each term, but to obtain a branching ratio

for the  $4l4l'$  states a summation over the entire Rydberg series must be performed, since it is assumed that only the  $4l4l'$  part of the eigenvector is populated initially and the 'average' stabilization ratio for each symmetry is obtained using

$$\langle R^r \rangle = \frac{\sum C_{44}^2 R^r}{\sum C_{44}^2} \quad (3)$$

with  $C_{44}^2$  the total amount of  $4l4l'$  character for a state and the summation is carried out over all bound states of the appropriate symmetry. If, for a particular symmetry, more than one  $4l4l'$  term exists, the average value assumes that all  $4l4l'$  terms are populated and are populated equally. For the highest  $4l4l'$  state, a  $1S^e$  term located above the  $N = 3$  threshold,  $R^r$  is determined in the same way as for the  $4l5l'$  states. It is noted that when the average radiative decay rate of the  $4l4l'$  terms within a particular symmetry is used in equation (1), the difference with the present results for the average rate (equation (3)) is a fraction of a per cent. This *a posteriori* justifies the method used in the study of  $O^{6+}$  (van der Hart *et al* 1994).

### 3. Results for the $4l4l'$ states

In table 1 we give the energies,  $E$ , before and the autoionization widths of the  $4l4l'$  states,  $A_{WI}^a$ , after inclusion of the interaction with the  $3lnl'$  series. The table shows also the 'preliminary' wavefunction compositions, i.e. without the interaction with the  $3lnl'$  series taken into account. In addition, the table shows the radiative decay rates for the preliminary states and the strength of their interaction with the  $3lnl'$  states,  $A_{3lnl'}^a$ , termed autotransfer or ATR rates by Bachau *et al* (1992). The preliminary  $4l4l'$  states have unambiguously  $n = 4$  character and the autoionization rate towards the lower-lying continua is well defined. After inclusion of the interaction with the  $3lnl'$  series, the preliminary  $4l4l'$  states are 'dissolved' in the  $3lnl'$  Rydberg series and it can be difficult to define the position and the width of a  $4l4l'$  state. As an illustration, the  $4l4l'$  character of the states in the  $1P^o$  symmetry is shown in figure 2. It can be seen that the two lowest  $4l4l'$  states are quite pure, with 84% and 51%  $4l4l'$  character, but the highest state, lying close to the  $N = 3$  threshold, has a maximum  $4l4l'$  contribution of only 13%.

The autoionization rates,  $A_{WI}^a$ , reported in table 1 are for those states which after diagonalization have the largest (total) amount of  $4l4l'$  character,  $C_{44}^2$ . (The actual  $C_{44}^2$  value is given in the last column of the table.) These states correspond fairly well to the centre of the resonance-like structure observed in the  $4l4l'$  composition of the states in the Rydberg series as a function of energy. However, the autoionization rates vary considerably over the resonance since the interference usually leads to an asymmetric Fano-type profile (see figure 3) along the Rydberg series. The autoionization rates reported in table 1 are thus dependent on which state is labelled  $4l4l'$  and to determine stabilization ratios the procedure described earlier, which takes the variation along the Rydberg series into account, is essential. Nevertheless, the individual  $A_{WI}^a$  values in table 1 are of interest, since they illustrate the magnitude of the autoionization rate compared to the autotransfer rate.

It can be seen from table 1 that the ATR rate towards the  $3lnl'$  states is much larger than the corresponding  $A_{WI}^a$  rate towards the  $(1, 2)l\epsilon l'$  continua, the difference ranging from a factor of three for the lowest  $1G^e$  state to a factor of 3000 for the highest  $1D^o$  state. This has been pointed out by Roncin *et al* (1993a) and is an important ingredient in the ATR mechanism. The low degree of mixing of  $3lnl'$  and  $4l4l'$  states for the unnatural parity states ( $\pi = (-1)^{L+1}$ ) is also noticeable, the smallest  $4l4l'$  component in such a state being



**Table 1.** Energies, autotransfer rates (see text) to  $3lnl'$  states,  $A_{3lnl'}^a$ , and total radiative decay rates,  $A^r$ , in  $\text{Ne}^{8+}$  for the singlet  $4l4l'$  terms obtained before inclusion of the interaction with the  $3lnl'$  Rydberg states, while autoionization rates,  $A_{W1}^a$ , and  $4l4l'$  contribution,  $C_{44}^2$ , refer to the states after inclusion of the interaction. The states are ordered by increasing energy within each  $LS$  symmetry. The main  $4l4l'$  components in column 2 are for the 'preliminary' states in the hydrogenic basis, i.e. taken from a calculation that does not include the interaction with  $3lnl'$  (see text).

$LS$	Main eigenvector components			$E$ (au)	$A_{3lnl'}^a$ ( $10^{12} \text{ s}^{-1}$ )	$A^r$ ( $10^{12} \text{ s}^{-1}$ )	$A_{W1}^a$ ( $10^{12} \text{ s}^{-1}$ )	$C_{44}^2$ (%)
$^1S^e$	49% $4s^2$	45% $4p^2$		-5.99289	127	0.681	16.5	87.4
	28% $4s^2$	56% $4d^2$		-5.90448	584	0.397	6.59	44.4
	15% $4s^2$	25% $4p^2$	55% $4f^2$	-5.74350	970	0.516	0.743	38.7
	22% $4p^2$	32% $4d^2$	34% $4f^2$	-5.48939	1.38	0.558	<sup>a</sup>	<sup>a</sup>
$^1P^o$	40% $4s4p$	53% $4p4d$		-5.94335	86	0.828	71.8	84.0
	35% $4s4p$	58% $4d4f$		-5.81411	939	0.527	3.86	50.9
	24% $4s4p$	39% $4p4d$	32% $4d4f$	-5.57497	136	0.674	0.571	12.6
$^1D^e$	42% $4s4d$	48% $4p^2$		-5.98002	141	0.858	1.21	44.4
	20% $4s4d$	63% $4d^2$		-5.90524	383	0.488	9.77	56.1
	25% $4p^2$	59% $4p4f$	11% $4d^2$	-5.86017	441	0.890	7.93	72.8
	11% $4s4d$	72% $4f^2$		-5.76855	462	0.374	1.22	44.0
$^1D^o$	23% $4s4d$	21% $4p4f$	18% $4d^2$	-5.61745	185	0.620	2.08	42.0
	86% $4p4d$	13% $4d4f$		-5.93630	135	0.871	1.02	92.5
	13% $4p4d$	86% $4d4f$		-5.82267	27.2	0.435	0.0095	96.9
$^1F^o$	64% $4s4f$	34% $4p4d$		-5.90343	280	0.415	8.89	56.0
	15% $4s4f$	15% $4p4d$	69% $4d4f$	-5.85070	505	0.429	5.35	61.1
	19% $4s4f$	49% $4p4d$	28% $4d4f$	-5.67204	486	0.595	2.92	37.5
$^1F^e$	99% $4p4f$			-5.87652	40.3	0.822	1.13	95.7
$^1G^e$	42% $4p4f$	56% $4d^2$		-5.91561	170	0.594	58.2	88.0
	18% $4p4f$	76% $4f^2$		-5.81252	781	0.361	3.76	56.7
	38% $4p4f$	37% $4d^2$	22% $4f^2$	-5.70231	703	0.513	6.02	36.3
$^1G^o$	99% $4d4f$			-5.87632	10.4	0.354	1.76	99.0
$^1H^o$	97% $4d4f$			-5.74434	1240	0.331	4.74	32.0
$^1I^e$	97% $4f^2$			-5.74800	1970	0.201	2.23	27.2

<sup>a</sup> Located above the  $N = 3$  threshold, thus  $A_{3lnl'}^a = A_{W1}^a$ .

92.5%. Comparing these numbers to those obtained in  $\text{O}^{6+}$  (van der Hart *et al* 1994), it can be seen that there is less mixing in  $\text{Ne}^{8+}$ , primarily because the  $4l4l'$  terms lie lower with respect to the Rydberg states in  $\text{Ne}^{8+}$  compared to  $\text{O}^{6+}$ . The radiative rates of the pure  $4l4l'$  states have increased according to the  $Z^4$  scaling law. The autoionization rates after inclusion of the coupling can be very different in the two ions since it depends on the position of the  $4l4l'$  states with respect to the  $3lnl'$  series which is different in  $\text{O}^{6+}$  and  $\text{Ne}^{8+}$ .

The asymmetry in the autoionization rates along a Rydberg series after inclusion of the interaction with the  $4l4l'$  terms, keeping the  $n^{-3}$  behaviour for the unperturbed series in mind, is a result of the interference between the decay rates of the  $3lnl'$  and  $4l4l'$  components. Destructive interference in the autoionization rate generally leads to an increase in the branching ratio for radiative decay, since the mixing usually has a negligible effect on the radiative decay. In figure 3 we show the widths of the states in the  $^1P^o$  symmetry as a function of  $n$ . At  $n = 10$ , there is a small discontinuity in the autoionization rate for the series with the largest autoionization width, which is caused by the lowest  $4l4l'$   $^1P^o$  state. The second  $4l4l'$  state is located near  $n = 12$  and in fact a change in autoionization rate

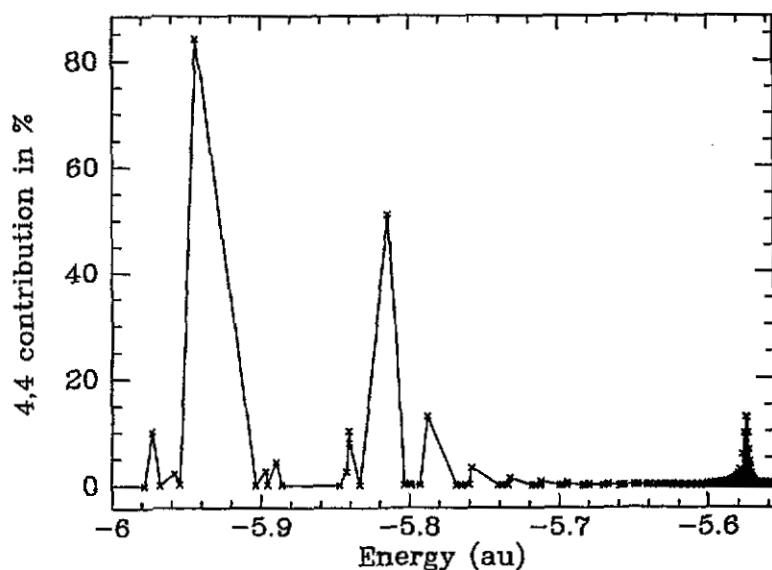


Figure 2. The  $4l4l'$  character of the  $1P^0$  Rydberg series in the free  $Ne^{8+}$  ion. There are three  $4l4l'$  states and five  $3lnl'$  Rydberg series with the  $1P^0$  symmetry.

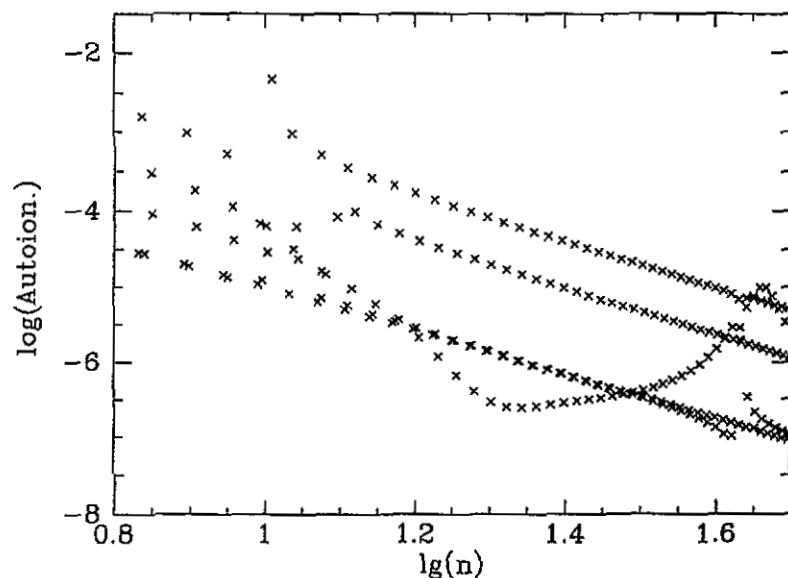


Figure 3. The width of the  $1P^0$  Rydberg states in  $Ne^{8+}$  as a function of  $n$  in the free atom.

is observed for the series with the second largest autoionization rate at this point. For the highest  $4l4l'$   $1P^0$  state, the interference with one series for which the autoionization rate does not follow the  $n^{-3}$  law at all is clearly visible on the figure. In addition, around  $n = 40$ , a Fano-type profile is seen in one of the series with a small autoionization rate. In this region, autoionization is already much less likely than radiative decay and the effect of destructive interference is marginal, whereas constructive interference leads to *less* stabilization. This is

one example of a general result of this and earlier studies, namely that detailed calculations, in which the positions of the  $4l4l'$  states are accurately described, are required for each ion.

The average stabilization ratios for each singlet symmetry are shown in table 2 and compared to the free-atom results for  $O^{6+}$  (van der Hart *et al* 1994) and to the static and dynamic results obtained for  $Ne^{8+}$  by Roncin (1993) using the approach described by Roncin *et al* (1993a). Since we assume that only the  $4l4l'$  basis states are populated, only average ratios for each symmetry have a physical significance because of the mixing and the same assumption lies behind the results due to Roncin (1993). Our  $O^{6+}$  results are included in order to show the  $Z$  dependence of the stabilization ratio. The variation in the ratios between the different symmetries shows that in order to obtain a stabilization ratio for the whole  $4l4l'$  configuration it is necessary to know the population distribution in the initial pick-up. It has been found in collisions of bare nuclei on He, that the majority of the population of the  $3l3l'$  states is found in states with high angular momentum (Bordenave-Montesquieu *et al* 1987, Mack *et al* 1989, Posthumus *et al* 1992). This result was not confirmed by Chetoui *et al* (1990) but, on the other hand, a weighting favouring high angular momenta did not significantly change the theoretical predictions for the overall stabilization ratio of the  $4l4l'$  complex in  $O^{6+}$  (van der Hart *et al* 1994) and table 2 shows the same for  $Ne^{8+}$  where the smallest overall ratio actually is found using a  $(2L + 1)^2$  weighting that emphasizes high angular momentum states. This is also evident from the individual results where the values for the  $^1S^e$ ,  $^1P^o$  and  $^1D^e$  terms are larger in  $Ne^{8+}$  than in  $O^{6+}$  while the opposite is found for the  $^1G^e$ ,  $^1H^o$  and  $^1I^e$  terms. On the other hand, very large differences in average stabilization ratios are observed between the different symmetries, which would make it possible to obtain nearly any value for the overall ratio by an appropriate choice of population distribution. A similar observation has been made by Bachau and Sánchez (1995). Thus more information is needed about the population distribution before it will be possible to make a realistic calculation for the overall stabilization ratio for the  $4l4l'$  states. With a statistical population distribution, an overall stabilization ratio of 29.2% is obtained for the singlet states, very close to the 29.7% found in  $O^{6+}$ .

Two factors are of importance for the  $Z$  dependence of the stabilization ratio, as mentioned already. The first is that radiative decay increases in importance due to the  $Z^4$  scaling law. This enhances radiative decay and favours an increase in the stabilization ratio. This effect can be appreciated from a comparison with the  $^1D^o$  symmetry, for which the  $4l4l'$  states remain very pure after inclusion of the interaction with the  $3lnl'$  series in  $Ne^{8+}$  as well as in  $O^{6+}$ . The decrease in the mixing is thus very small and so is the effect on the autoionization rates. Thus for this symmetry the  $Z^4$  increase in radiative decay dominates over the increase in the probability for autoionization, as can be seen from table 2.

The second effect, the relative lowering of the  $4l4l'$  energy in the  $3lnl'$  series, has in general the opposite consequence. For lower  $n$  values in the Rydberg series, the energy spacing between adjacent levels is larger, while the ATR rates remain fairly constant, so the  $4l4l'$  character will be smeared out over a smaller number of states and generally the  $4l4l'$  state will be less perturbed. At the same time, the Rydberg components also have a larger autoionization rate, due to  $n^{-3}$  scaling. Thus autoionization is favoured but detailed calculations are required to determine the effect of the interference. The final result in  $Ne^{8+}$  is that the overall stabilization ratio is basically unchanged compared to  $O^{6+}$ .

Considering the individual symmetries, we see that for most of those with the same number of states below the  $N = 3$  threshold in both ions, stabilization is reduced when going from  $O^{6+}$  to  $Ne^{8+}$ . The exceptions are the  $^1D^o$  symmetry, which has been described above, and the  $^1S^e$  symmetry. For the  $^1S^e$  symmetry, one state is located above threshold in

Table 2. Branching ratios for radiative decay for the  $4l4l'$  states with the interaction with the Rydberg series taken into account. Ratios are given averaged over all states with the same  $LS$  symmetry assuming that only the  $4l4l'$  basis states are populated initially. The number of states in each  $LS$  symmetry is also indicated. At the bottom of the table overall values are given, obtained with the weighting factors given in the first column. The close-coupling results have been obtained by Roncin (1993).

$LS$	Number of states	$(R^l)$ B-spline		$(R^l)$ Close-coupling	
		$O^{6+}$ (%)	$Ne^{8+}$ (%)	$Ne^{8+}$ stat. (%)	$Ne^{8+}$ dyn. (%)
$^1S^e$	4	21.2	24.2	16.0	22.6
$^1P^o$	3	13.8	35.6	28.5	46.1
$^1D^e$	5	17.3	27.5	18.3	27.9
$^1D^o$	2	64.2	72.9	58.4	76.2
$^1F^o$	3	12.6	17.9	7.3	18.1
$^1F^e$	1	53.4	44.2	17.8	97.3
$^1G^e$	3	27.3	15.3	10.3	19.1
$^1G^o$	1	27.9	17.5	9.4	72.6
$^1H^o$	1	38.0	27.3	17.9	96.8
$^1I^e$	1	54.5	44.2	20.0	16.3
Weighting factor				Average	
1		26.4	30.0	19.8	38.1
$(2L + 1)$		29.7	29.2	18.1	40.2
$(2L + 1)^2$		32.5	28.4	16.5	40.4

both ions and this 'anti-Wannier' state has a very small autoionization rate. Autoionization of this state is hardly influenced by the relative lowering of the  $4l4l'$  complex and only the increase in radiative decay is important. The increase in stabilization for the state above threshold more than compensates for the decrease in stabilization due to the states below threshold. However, in general the decrease in dispersion is more important than the increase in the radiative decay rates as observed for the other states of this type.

The  $^1P^o$ ,  $^1D^e$  and  $^1F^o$  symmetries with states that lie above the  $N = 3$  threshold in  $O^{6+}$ , but below in  $Ne^{8+}$ , show an increase in the average stabilization ratio, because the states, which are just below threshold in  $Ne^{8+}$ , are dispersed in the Rydberg series in  $Ne^{8+}$  and consequently have a large stabilization ratio. The smallest increase, 5%, is observed for the  $^1F^o$  symmetry, since in  $O^{6+}$  the highest state is just above threshold and in  $Ne^{8+}$  this state therefore lies furthest below threshold. On the other hand, the average stabilization ratio increases by a factor of 2.6 for the  $^1P^o$  series and by a factor of 1.6 for  $^1D^e$ . The  $^1P^o$  series has the second highest average stabilization ratio of the terms with natural parity. The high degree of stabilization for these low angular momenta is the reason that the  $(2L + 1)^2$  weighting reduces the overall stabilization ratio as noted above.

The comparison in table 2 with the static results obtained by Roncin (1993) shows that there is only a moderate agreement between the two static methods with the present results the higher ones for all symmetries. A similar result was found for  $N^{5+}$  (van der Hart and Hansen 1994). In the close-coupling calculations performed by Roncin and co-workers (Roncin *et al* 1993a, b, Roncin 1993), decay of the  $3ln'l'$  and  $4l4l'$  components was taken into account without including interference. This was identified as the reason for the differences in the average stabilization ratios in  $N^{5+}$  and figure 3 shows interference also to be significant in  $Ne^{8+}$  so that this conclusion gains further support. Interference would

also explain why the difference is so large for the highly dispersed  $4f^2\ ^1I^e$  term. Since the difference between the two sets of results is fairly independent of the symmetry, the difference in the overall stabilization ratio is about 10%, independent of weighting.

Roncin (1993) also determined stabilization ratios for  $Ne^{8+}$  including the ATR mechanism. The dynamic and static close-coupling results differ considerably. For most symmetries a larger stabilization ratio is found in the dynamic approach with increases of factors of eight, for  $^1G^o$ , and six, for  $^1F^e$  and  $^1H^o$ , but for  $^1I^e$  a decrease is observed. The latter can be explained (van der Hart and Hansen 1994) by the large mixing with the lower (autoionizing) part of the  $3lnl'$  series in the beginning of the process, which effectively transfers the  $4l4l'$  population well before reaching the higher Rydberg states. The transfer rate is, as can be seen from table 1, by far the largest for the  $^1I^e$  state, and this effect is thus most prominent for this symmetry.

The large increase for the  $^1G^o$ , the  $^1F^o$  and, in particular, the  $^1H^o$  symmetries are more difficult to understand. It is surprising that very different stabilization ratios are obtained for the  $^1H^o$  and the  $^1I^e$  symmetries in the dynamic calculation, since these states lie close to each other in energy and both have a large interaction with the  $3lnl'$  Rydberg series. However, in the dynamic calculation the interaction with only one Rydberg series is taken into account and the choice of series is somewhat arbitrary (Roncin 1993) so that the difference between the two terms probably is artificial. As in  $O^{6+}$ , the difference with our overall value is about 10% but this time our value is the smaller one. However, we also ascribe this difference primarily to the neglect of interference in the ATR procedure, as well as the arbitrary choice of Rydberg series mentioned above.

This conclusion is supported by the recent publications of more accurate ATR results by Sánchez and Bachau (1995) and Bachau and Sánchez (1995). Sánchez and Bachau (1995) give explicit results only for the five  $^1D^e$  terms. They report a  $\langle R^r \rangle$  value of 30% to be compared with our free atom value of 27.5% and with the 27.9% given by Roncin *et al* (1993b). Whether the difference(s) can be ascribed to the ATR effect is not entirely clear since the calculations, the ATR effect excepted, are not entirely equivalent. For example in contrast to us, Sánchez and Bachau (1995) neglect the radiative decay of the pure  $4l4l'$  states. However, more significantly, Bachau and Sánchez (1995) report an overall value of 25% for all singlets assuming the same population independent of  $L$ . This should be compared to our value of 30% (table 2) and to the value of 38% obtained by Roncin (1993). The absolute accuracy of the average values is expected to be better than that for the individual values allowing us to conclude that the ATR mechanism also in this case does not lead to an increase in stabilization.

We have not considered triplet states here, for which Roncin (1993) in the dynamic approach finds a much larger degree of stabilization than for singlets, whereas in the static approach the same overall stabilization ratio for singlet and triplet states is found, in accordance with the results for  $O^{6+}$  (van der Hart *et al* 1994). We have performed a calculation for the  $^3H^e$  symmetry in the free  $Ne^{8+}$  ion and found a stabilization ratio of 75.5%, compared to 72.2% in  $O^{6+}$  and 44.7% in the  $Ne^{8+}$  ion determined by Roncin (1993). This result shows that, as in  $O^{6+}$ , triplet states in  $Ne^{8+}$  can also have large stabilization ratios. The  $^3H^e$  term is of particular interest because of its high angular momentum, which could be favoured at higher collision velocities (Posthumus and Morgenstern 1990).

#### 4. A semi-static approach

In order to throw light on the differences between the static and the dynamic approach, we have carried out a series of calculations in which some dynamical aspects of the capture

process are taken into account. The approach is less accurate than the time-dependent close-coupling method used by Roncin *et al.* (1993a), but on the other hand some of the assumptions behind the latter are explored and found to be significant for the result. Also interference between the eigenvector components for the autoionization decay is included, which is not the case in the calculations reported by Roncin *et al.* The idea can be understood from figure 4, which shows on the left a 'real' energy level diagram as a function of the internuclear distance and on the right the approximation to the level diagram which is used here to model the capture process as a two-step process: initial states are populated during the collision and these states are suddenly transformed into the free-atom states when the influence of the target has waned.

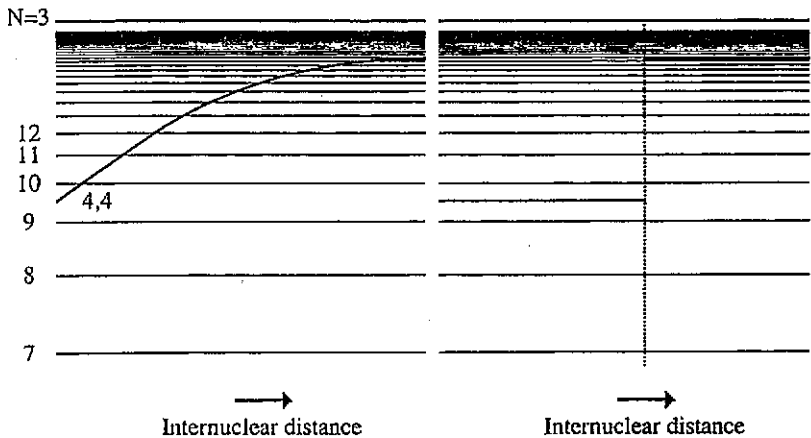


Figure 4. The energy diagram for a  $4l4l'$  term as a function of internuclear distance on the 'way out' of the collision (left) and the two-step semi-static approximation to this energy level diagram (right).

It is assumed that the initial capture into  $4l4l'$  takes place at an internuclear distance  $R_c$ , which is so small that the charge of the (now) doubly-ionized target has a considerable influence on the projectile energy levels. We assume that the single-electron energies of the projectile states with quantum numbers  $n$  and  $l$  are shifted by amounts given by

$$\Delta E = (1 - W_0) \frac{-(Z+1)^2 + (Z-1)^2}{2n^2} + W_0 \frac{-2}{R} \quad (4)$$

with

$$W_0 = \exp\left(\frac{-R_0^2(l)}{2R_c^2}\right) \quad (5)$$

where

$$R_0^2(l) = (5n^2 - 3l(l+1) + 1) \frac{n^2}{2(Z-1)^2} \quad (6)$$

is the expectation value of  $r^2$  for a hydrogenic orbital with angular momentum  $l$  in a hydrogen-like ion with charge  $Z-1$ . In principle equation (4) is valid for the last electron but we apply it to both, although we note that the first term in practice is close to zero for (the first) electron with  $n \leq 4$ . For low  $n$  values, the asymptotic limit of equation (4) is  $-2/R$  and for high  $n$  values  $-[(Z+1)^2 - (Z-1)^2]/(2n^2)$ . For low  $n$  values the field induced by the target can be considered as a linear Stark field and our treatment for these

states is similar to the treatment in the ATR approach (Bachau *et al* 1992, Roncin *et al* 1993a, b). However, in addition, equation (4) introduces a shift for the Rydberg states, since for internuclear distances that are small compared to the mean radius of the Rydberg orbital, the charge of the ionized target can be considered as contributing to the central charge. This effect is not introduced in the ATR model used by Roncin *et al* (1993a, b), but it turns out to be significant.

Its importance is demonstrated by a small time-dependent close-coupling calculation of the type used by Roncin *et al* (1993a). In this model calculation for the  $1I^e$  symmetry in  $O^{6+}$ , the interaction between the  $4l4l'$   $1I^e$  term and a  $1I^e$  Rydberg series is studied where the interaction between  $4l4l'$  and  $3lnl'$  is determined from the autotransfer width and has been chosen to exhibit the proper  $n$  dependence. It is assumed that initially only the  $4l4l'$  basis state is populated. In contrast to Roncin *et al* (1993a), no subsequent decay is included in the calculations. We have performed two calculations, one in which the energy of the Rydberg series is constant and one in which the Rydberg energy is allowed to vary with internuclear distance. In both cases a Stark shift equal to  $-2/R$  is included. The result of the calculation is shown in figure 5, with on the left the magnitude of the  $4l4l'$  component in the time-dependent wavefunction. The  $4l4l'$  amplitude is proportional to the population. It can be seen that in the calculation without Rydberg shift (top) almost no population is present in the  $4l4l'$  state after a very short time, but upon inclusion of the Rydberg shift a significant  $4l4l'$  population survives the collision. The effect of the shift is that the  $4l4l'$  state starts 'higher' in the Rydberg series. The right-hand side of figure 5 shows the time dependence of the size of the  $3l1l'$  component, confirming that the higher  $3lnl'$  states pick up significantly more population in the 'Rydberg shifted' case, while in the other case most population ends up in lower Rydberg states. The  $4l4l'$  state passes quickly through the low Rydberg states and afterwards the interaction is weak due to the energy difference between the states so that population cannot flow back, while the latter is possible when the state passes the higher Rydberg states (compare the lower left panel in figure 5). The main effect is to enhance radiative decay, since higher Rydberg levels are populated.

Using expression (4) for the energy shift, the  $4l4l'$  states are lowered in energy with respect to the  $3lnl'$  states during the collision. In the semi-static calculation, which we describe now, the diagonalization of the CI matrix with the shift included gives the level structure at the moment of capture. This can differ considerably from the eigenfunctions in the free atom as realized by Bachau *et al* (1992). The initial population of each of the shifted states is modelled by the total amount of  $4l4l'$  character in the state.

If the collision happens very fast, the difference between the static and the dynamic results will disappear, since the  $4l4l'$  state will pass through the Rydberg series without having 'time' to interact before it comes 'to rest' in the free atom. Thus the largest difference between static and dynamic results should be found at low energy and the semi-static results obtained here provide a measure of the maximum difference between the two approaches. In the semi-static approximation, the initial wavefunction is projected onto the wavefunctions in the free atom signifying that once the initial wavefunction is formed it cannot follow the changes in the potential.

Two sets of calculations are described. The most extensive is based on the use of  $l = 2$  to calculate the value of  $W_0$ , independent of the actual  $l$  value of the outer electron. This is called the 'degenerate Rydberg approach', since all Rydberg states with the same  $n$  value are shifted by the same amount. The second set is based on using the proper  $l$  value. We will first describe the results obtained with the degenerate Rydberg approach.

We show in figure 6 the composition of the  $4f^2$  and the  $3lnl'$  states for the  $1I^e$  symmetry in  $Ne^{8+}$  in the static and the semi-static approaches, respectively. The latter results are

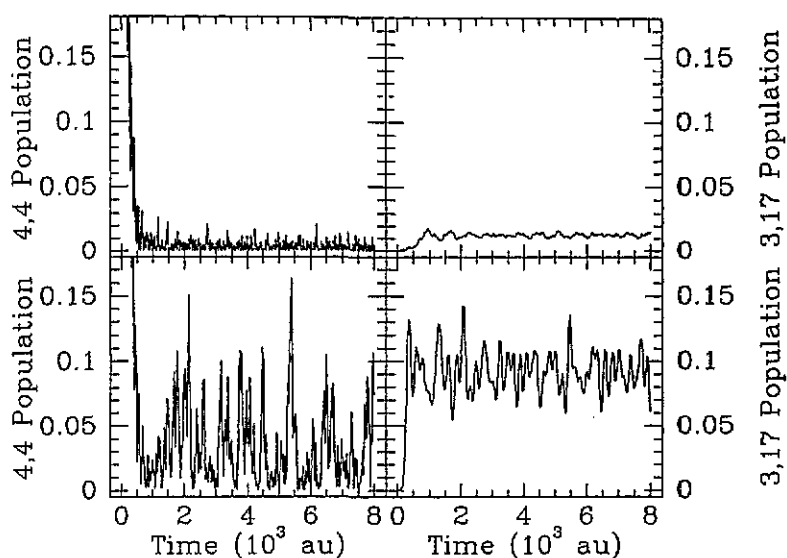


Figure 5. Time dependence of the  $4l4l'$  amplitude during the traverse of the Rydberg series obtained in the close-coupling calculation for the  $1I^e$  symmetry described in the text. In the upper panels, the energies of the Rydberg states remain constant during the collision, whereas in the lower ones a shift of the Rydberg states has been included as explained in the text. The left side shows the size of the squared  $4l4l'$  amplitude, while the right side shows the squared  $3l17l'$  amplitude.

obtained for a capture radius  $R_c$  of 5 au. In the present approximation the  $4l4l'$  amplitude is proportional to the population of the levels after the collision. In the semi-static approach a large amount of the initial population is transferred to the Rydberg series at about  $n = 9$ , with additional population over a region corresponding to the mixing in the free atom. For this higher Rydberg region, the  $4l4l'$  'lineshape' is similar to the one found in the free atom.

The difference in final-state population affects the stabilization ratio of the  $1I^e$  series. In table 3 we show stabilization ratios obtained using several capture radii for the  $Ne^{8+}$  ion and, for comparison, the  $O^{6+}$  ion. For the approximation to be useful, the dependence on capture radius must be small. In real collisions, a distribution of capture radii populating the  $4l4l'$  levels can be expected and an average over capture radius needs to be determined.

The results obtained show a larger variation with capture radius for  $Ne^{8+}$  than for  $O^{6+}$ . For  $Ne^{8+}$ , there is a tendency for the stabilization ratio to increase with larger  $R_c$ . The reason is that, for larger  $R_c$ , the first degeneracy is with a higher state in the Rydberg series, which has a smaller probability for autoionization. This effect is less pronounced for  $O^{6+}$  where the  $4l4l'$  state starts higher in the Rydberg series.

Although the final population distributions are very different, as illustrated in figure 6, table 3 shows that the stabilization ratio does not change more than 10% for  $Ne^{8+}$ . This means that the result of the semi-static approximation is close to the free atom value and, for small  $R_c$ , usually smaller than the static values, in agreement with our earlier observation that it is capture into low, i.e. autoionizing levels, that is boosted by the ATR mechanism (van der Hart and Hansen 1994). This agrees with the more accurate ATR calculations by Bachau and Sánchez (1995) who, as mentioned already, report an overall stabilization ratio which is 5% smaller than ours. We note that Sánchez and Bachau (1995) find a small variation in stabilization with capture radius but in the absence of a Rydberg series shift.



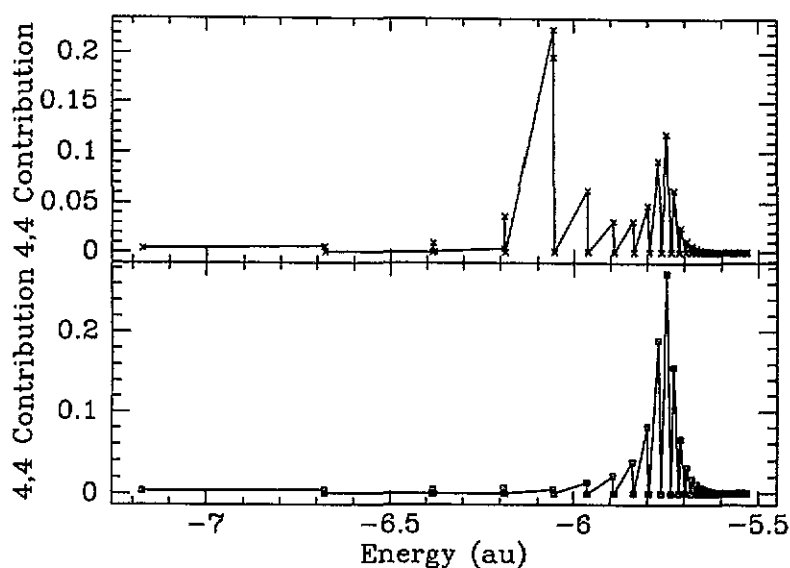


Figure 6. The squared  $4l4l'$  amplitude in the perturbed  $1I^e$  Rydberg states in  $Ne^{8+}$  in the semi-static approach (top) and in the free atom (bottom). The energy  $-6.2$  au corresponds to  $n = 8$ .

Table 3. Stabilization ratios for the  $1I^e$  series in the  $O^{6+}$  and the  $Ne^{8+}$  ion using the semi-static approach with different capture radii and different energy shifts as explained in the text. In column 3,  $n$  indicates the degenerate Rydberg approach, whereas  $n, l$  indicate the approach with an  $l$  dependent energy shift for the Rydberg series. The dynamic results have been obtained by Roncin (1993).

Ion	Method	Dependence	Capture radius (au)	Stabilization ratio (%)
$O^{6+}$	Static			54.5
	Semi-static	$n$	5	38.0
	Semi-static	$n$	6	40.2
	Semi-static	$n$	7	40.2
	Semi-static	$n$	8	39.8
$Ne^{8+}$	Static			44.2
	Dynamic			16.3
	Semi-static	$n$	5	42.0
	Semi-static	$n$	6	41.8
	Semi-static	$n$	7	44.6
	Semi-static	$n$	8	45.9
	Semi-static	$n, l$	5	47.7
	Semi-static	$n, l$	6	52.6
	Semi-static	$n, l$	7	51.6
Semi-static	$n, l$	8	58.6	

It is not obvious how to extrapolate the  $1I^e$  results to other symmetries. One reason is that the  $1I^e$  symmetry is more weakly autoionizing than the other symmetries because of

the  $l^{-5}$  scaling law for autoionization rates (Cooke and Gallagher 1979). Also the  $^1I^e$  term interacts strongly with the Rydberg series, whereas this is not the case for all other terms. The population of the low Rydberg states may, therefore, depend more on the capture radius in other cases.

We now pass to the calculations involving the use of the actual  $l$  value in equation (5) instead of  $l = 2$ . The consequence is that the Rydberg manifold is split significantly and the result of this splitting is that the mixing of the  $3lnl'$  Rydberg states with the same  $n$  value decreases. This usually reduces the interaction with the  $4l4l'$  terms. Another feature is that states with high angular momentum are closer to the core in the hydrogenic approximation and experience a larger energy-lowering shift than  $d$  electrons. The  $4l4l'$  term can therefore be degenerate with higher  $n$  states than in the degenerate Rydberg case. Both effects can be seen in figure 7.

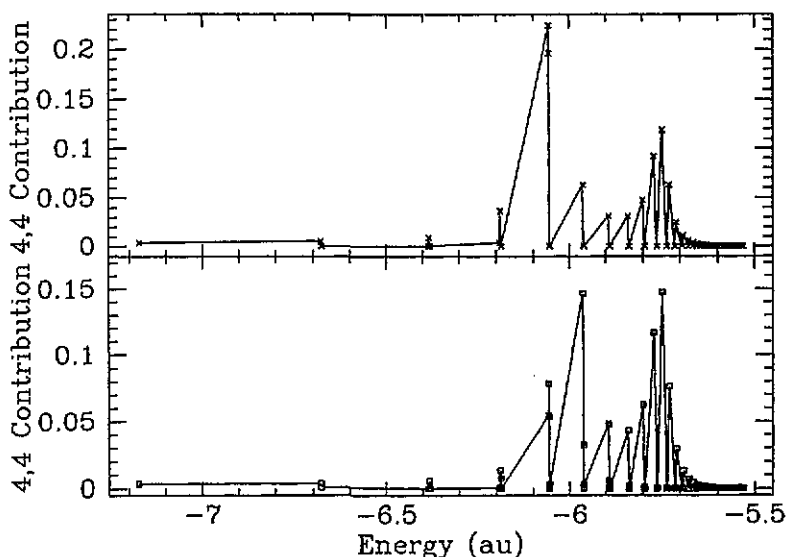


Figure 7. The squared  $4l4l'$  amplitude in the perturbed  $^1I^e$  Rydberg states in  $\text{Ne}^{8+}$  as a function of energy in the semi-static approach with an  $l$  dependence in the Rydberg shift (bottom), compared to the squared  $4l4l'$  amplitude in the  $^1I^e$  Rydberg states in the semi-static approach with an  $l$ -independent shift (top). The energy  $-6.2$  au corresponds to  $n = 8$ .

The effect of the splitting of the Rydberg levels is seen for the  $n = 9$  manifold, the most important one in the degenerate Rydberg case, for which two states contribute 42% to the population, but in the non-degenerate case three states contribute, adding up to a total of 18%. For the neighbouring manifolds, there is only one  $3lnl'$  series populated in the degenerate Rydberg case, whereas there are several series populated in the non-degenerate case. The increase in the population of the  $n = 10$  manifold in the non-degenerate Rydberg case is also clearly visible. This is due to the larger lowering of the energy of states with large  $l$  values.

To study the  $Z$  dependence of the stabilization ratio in the semi-static approach, we have also examined the  $^1I^e$  symmetry in  $\text{O}^{6+}$  as mentioned earlier. The results of this calculation are included in table 3. Figure 6 shows that in  $\text{Ne}^{8+}$  the additional peak appears at a principal quantum number  $n = 9$  in the Rydberg series for  $R_c = 5$  au, and this is also the case for  $\text{O}^{6+}$ . However, since radiative decay is less important for  $\text{O}^{6+}$  than for

Ne<sup>8+</sup>, table 3 shows a decrease of 15% in the stabilization ratio for O<sup>6+</sup> in the semi-static approach, while very little change is found for Ne<sup>8+</sup>. This confirms that dynamic effects on the stabilization ratio are smaller in Ne<sup>8+</sup> than in O<sup>6+</sup>, but in neither case do such effects lead to an increase in stabilization. The original suggestion by Bachau *et al* (1992) was that the ATR mechanism should be particularly effective when the 4*l*4*l'* states lie high in the 3*lnl'* series, i.e. for low *Z*. Here, in contrast, it is found that due to the ATR mechanism radiation gains in importance with increasing *Z*. However, we have mentioned already that we consider the free-atom values a sort of upper limit to the ATR effect and we believe that this is also the case in Ne<sup>8+</sup>. This view is supported by the calculations reported by Bachau and Sánchez (1995), mentioned earlier, and we believe that the opposite result obtained by Roncin *et al* (1993a) is due to the approximations involved in this calculation. Thus we conclude that the global effect of the ATR is to *reduce* stabilization. However, we note that the opposite might be true for specific terms because of the interference in the autoionization rate which does depend on the details of the interaction.

## 5. Results for the 4*l*5*l'* states

In table 4 energies, autoionization widths towards the 3*lel'* continua, radiative decay rates and branching ratios for radiative decay are given for all singlet 4*l*5*l'* terms. These terms are all located above the *N* = 3 threshold and autoionize preferentially towards the *N* = 3 limit. The radiative decay rates are, as mentioned, calculated to the lowest 15 states of each symmetry below the *N* = 2 and the *N* = 1 thresholds. Also decay towards 3*lnl'* has been considered except that some 3*l*6*l'* states were omitted. Since the radiative decay rates scale with ( $\Delta E$ )<sup>3</sup>, the most important decays are towards the 1*snl* states. Eigenvector compositions are not reported; they are similar to the eigenvector compositions of the 4*l*5*l'* states in the O<sup>6+</sup> ion reported recently (van der Hart *et al* 1994).

The largest autoionization rate, slightly smaller than 10<sup>15</sup> s<sup>-1</sup>, is found for the lowest <sup>1</sup>F<sup>e</sup> state, whereas the smallest autoionization rate is obtained for the highest <sup>1</sup>D<sup>o</sup> state with a decay rate of just over 10<sup>10</sup> s<sup>-1</sup>. Within <sup>1</sup>D<sup>o</sup>, the autoionization rates differ by four orders of magnitude, whereas the radiative decay rates 'only' differ by a factor of three. This justifies our assumption that it is more important to have an accurate description of autoionization than of radiative decay.

Table 4 shows, that for only six (among 60) states the branching ratio for radiative decay is above 10%, of which four (of 20) have unnatural parity and only two (of 40) natural parity. This confirms that radiative decay is much more important for states with unnatural parity, as also found for O<sup>6+</sup>. The highest radiative decay rate is found for the lowest <sup>1</sup>P<sup>e</sup> state with a decay rate of just over 10<sup>12</sup> s<sup>-1</sup>.

In table 5 the stabilization ratios for each 4*l*5*l'* symmetry are given and compared to the values obtained for O<sup>6+</sup>. For all symmetries the importance of radiative decay increases from O<sup>6+</sup> to Ne<sup>8+</sup>. For symmetries with a branching ratio less than 12% in O<sup>6+</sup>, the branching ratio increases by a factor which can be explained by the *Z*<sup>4</sup> scaling law. On the other hand, for <sup>1</sup>P<sup>e</sup>, <sup>1</sup>D<sup>o</sup> and <sup>1</sup>F<sup>e</sup> this does not apply, since the branching ratios for these symmetries are dominated by one state with a very large stabilization ratio and radiative stabilization does not follow a *Z*<sup>4</sup> scaling law in such cases. The overall stabilization ratio for the complex is 6.2% compared to 2.6% for O<sup>6+</sup>. Gaboriaud *et al* (1993) and Roncin *et al* (1993b) have published experimental values for O<sup>8+</sup> on Ar and Ne<sup>10+</sup> on Ne, respectively. In both cases, the 4*l*5*l'* manifold is preferentially populated in double capture. However, the observed stabilization ratios are very different; 11% in oxygen compared to 3% in neon. Neither value agrees with the calculated value, but what is more surprising is that also

**Table 4.** Total energies, autoionization rates, radiative decay rates and radiative branching ratios for the  $4l5l'$  states in  $Ne^{8+}$ . The states are ordered according to increasing energy within each  $LS$  symmetry.

$LS$	$E$ (au)	$A^a$ ( $10^{12} s^{-1}$ )	$A^r$ ( $10^{12} s^{-1}$ )	$R^r$ (%)	$LS$	$E$ (au)	$A^a$ ( $10^{12} s^{-1}$ )	$A^r$ ( $10^{12} s^{-1}$ )	$R^r$ (%)
$^1S^e$	-4.914 01	79.8	0.519	0.6	$^1F^o$	-4.918 80	6.64	0.619	8.5
	-4.837 08	422.9	0.293	0.1		-4.872 95	5.35	0.247	4.7
	-4.730 37	585	0.364	0.1		-4.848 86	139	0.323	0.2
	-4.599 80	1.62	0.469	22		-4.846 47	55.4	0.413	0.7
$^1P^o$	-4.935 88	3.72	0.633	15	-4.806 01	350	0.307	0.1	
	-4.885 15	12.5	0.472	3.6	-4.769 12	77.4	0.395	0.5	
	-4.878 75	216.2	0.648	0.3	-4.704 67	249	0.395	0.2	
	-4.805 00	10.0	0.434	4.2	-4.663 05	40.1	0.440	1.1	
	-4.785 04	651.7	0.386	0.1	$^1F^e$	-4.894 83	5.56	0.455	7.6
	-4.657 18	6.36	0.238	3.6		-4.869 46	11.1	0.423	3.7
$^1P^e$	-4.642 46	64.1	0.519	0.8	-4.835 41	27.7	0.587	2.1	
	-4.916 19	5.86	1.218	17.2	-4.810 68	0.036	0.214	86	
	-4.856 54	11.3	0.602	5.1	-4.779 97	9.19	0.346	3.6	
$^1D^e$	-4.767 71	0.19	0.355	65	$^1G^e$	-4.864 73	67.1	0.532	0.8
	-4.907 01	8.04	0.383	4.5		-4.864 37	30.8	0.445	1.4
	-4.900 36	100.3	0.649	0.6	-4.826 12	125	0.177	0.1	
	-4.843 31	244.5	0.335	0.1	-4.788 44	282	0.218	0.1	
	-4.834 12	10.6	0.389	3.5	-4.745 03	437	0.345	0.1	
	-4.818 83	329	0.680	0.2	-4.676 56	94.0	0.397	0.4	
	-4.757 78	243	0.255	0.1	$^1G^o$	-4.848 05	4.41	0.345	7.3
	-4.691 86	109.8	0.428	0.4		-4.840 15	9.21	0.253	2.7
$^1D^o$	-4.654 64	40.3	0.474	1.2	-4.823 85	18.1	0.601	3.2	
	-4.889 98	9.30	0.563	5.7	-4.790 85	12.0	0.221	1.8	
	-4.874 10	93.3	0.652	0.7	$^1H^o$	-4.872 35	23.1	0.317	1.4
	-4.817 09	6.90	0.412	5.6		-4.802 06	215	0.470	0.2
	-4.799 54	16.1	0.320	1.9	-4.740 38	619	0.180	0.0	
	-4.744 38	0.011	0.213	95	-4.684 66	113	0.408	0.4	
					$^1H^e$	-4.833 65	8.57	0.159	1.8
						-4.817 52	0.373	0.243	39
				$^1I^e$	-4.795 01	921	0.190	0.0	
					-4.698 45	300	0.220	0.1	
				$^1J^o$	-4.825 24	45.9	0.113	0.2	
					$^1K^o$	-4.696 42	378	0.117	0.0

the trend is different. Roncin *et al* (1993b) have commented that this difference between oxygen and neon is not understood. However, the variation in stabilization ratio between different terms means that also this result in principle can be understood if the population distribution differs between the two. The possibility that this is so was mentioned by Roncin *et al* and it would be interesting to see if it would be possible to make a more detailed analysis of the population distribution for the  $4l5l'$  terms in the two ions.

## 6. Conclusions

Despite the large amount of work performed for the  $4l4l'$  states recently, the puzzle behind the large observed radiative stabilization ratios is still not solved. The overall stabilization ratio for the singlet  $4l4l'$  terms in the free atom, assuming a statistical population distribution, is 29%, considerably smaller than the experimental results although significantly larger than

**Table 5.** Branching ratios for radiative decay for the  $4l5l'$  states in  $O^{6+}$  and  $Ne^{8+}$ . Ratios are given averaged over all states with the same  $LS$  symmetry. The number of states within each  $LS$  symmetry is shown as well

$LS$	Number of states	$\langle R^r \rangle$		$LS$	Number of states	$\langle R^r \rangle$	
		$O^{6+}$ (%)	$Ne^{8+}$ (%)			$O^{6+}$ (%)	$Ne^{8+}$ (%)
$^1S^e$	4	2.6	5.7	$^1G^e$	6	0.3	0.5
$^1P^o$	7	1.6	3.9	$^1G^o$	4	1.9	3.8
$^1P^e$	3	18	29	$^1H^o$	4	0.2	0.5
$^1D^e$	8	0.7	1.3	$^1H^e$	2	11	20
$^1D^o$	5	19	22	$^1J^e$	2	0.0	0.1
$^1F^o$	8	0.9	2.0	$^1J^o$	1	0.1	0.2
$^1F^e$	5	17	21	$^1K^o$	1	0.0	0.0

if the interaction with the  $3lnl'$  series is neglected.

The assumption of a statistical population distribution is not likely to be correct and a non-statistical population distribution is likely to be an essential element in the final explanation. However, other elements have also to be considered. The ATR mechanism has been proposed as one of these, but we have shown that this effect in the formulation of Roncin *et al* (1993a) is generally too effective and leads to a reduction in the stabilization obtained for the free atom. In  $Ne^{8+}$  Roncin *et al* (1993b) appeared to have found an element where this is not the case. We believe that this result is an artefact of the calculational procedure, but we agree with Roncin *et al* that the reduction in stabilization due to ATR is smaller in  $Ne^{8+}$  than in the lighter systems and our results allow us to explain why this is so: in  $Ne^{8+}$  the transfer to low Rydberg states is less effective in inducing autoionization than in  $O^{6+}$  because the  $Z^4$  scaling of the radiative decay rates ensures a higher degree of stabilization for such states. Thus the ATR mechanism, which originally was assumed to be particularly effective at low  $Z$ , in fact seems to be more effective at larger  $Z$ . Nevertheless, we conclude that the mechanism on average does lead to smaller degrees of stabilization than is found in the free atom.

We have also shown that the ATR model is sensitive to the precise assumptions about the difference in energy between the  $4l4l'$  term and the Rydberg series as a function of internuclear distance. Introducing an energy dependence also for the Rydberg series leads to a decrease in the transfer to lower (autoionizing) Rydberg states, which will lead to a higher degree of stabilization than in the model employed by Roncin *et al* (1993a). To increase the probability for stabilization Roncin *et al* (1993a, b) have emphasized the Kazansky effect (Kazansky 1992, Kazansky and Roncin 1994) in which the  $l$  values of the captured electrons are increased by the field of the receding target and this mechanism can lead to a real increase in stabilization. Also Martin *et al* (1994) have emphasized the importance of the  $l$  distribution for the stabilization.

A different aspect is that recent experimental investigations of collisions involving  $N^{7+}$  and  $Ne^{10+}$  ions show that  $3lnl'$  states with  $n$  up to at least nine are populated (Bordenave-Montesquieu *et al* 1994, Frémont *et al* 1994, de Nijs *et al* 1994) while Wu *et al* (1994) have reported evidence for the population of  $2lnl'$  states with  $n > 10$  in collisions involving  $N^{7+}$  or  $O^{7,8+}$  and He. De Nijs *et al* have pointed out that the lower  $3lnl'$  states in  $N^{7+}$  lie too low to be populated via the ATR mechanism in collisions with Ar. This means that the possibility of populating the  $3lnl'$  states in some other manner has to be considered more

seriously.

One motive behind this work was to obtain an idea about the dependence on the nuclear charge. At first sight a simple  $Z$  behaviour could be expected, since for neutral helium, in which all  $4l4l'$  states lie above the  $N = 3$  threshold, autoionization is the dominant decay process, whereas in the (non-relativistic) high  $Z$  ions, radiation is expected to be dominant due to the  $Z^4$  scaling of radiation. However, for intermediate  $Z$  we have found that the transition from low to high  $Z$  is not smooth. Instead, there generally is an abrupt increase in the radiative decay rate, when a state gets below the  $N = 3$  threshold. With increasing  $Z$ , the probability for radiation decreases again, due to the decrease in the mixing with the Rydberg series when the  $4l4l'$  state lies lower in the  $3lnl'$  Rydberg series, while, finally, the radiative rates increase again, due to the  $Z^4$  scaling. The highest  $4l4l'$  state in  $Na^{9+}$  still lies above the  $N = 3$  threshold and it can therefore be anticipated that, although radiation is enhanced by a factor of 1.5, autoionization will be more important in  $Na^{9+}$  than in  $Ne^{8+}$ .

For the  $4l5l'$  states, an overall stabilization ratio of 6% is obtained, larger than in the equivalent states in  $O^{6+}$ , in reasonable agreement with a  $Z^4$  scaling law. Assuming a statistical population distribution, also this result does not agree with recent observations. On the other hand, since calculations for the  $4l5l'$  manifold should be the more accurate, a detailed comparison of theory with experiment for this manifold is attractive in order to test the assumption of a statistical population distribution.

## Acknowledgments

We are indebted to H Bachau, A Bordenave-Montesquieu, F Frémont, H Merabet, R Morgenstern, N Stolterfoht, W Wu and, in particular, P Roncin for sending us results ahead of publication and for stimulating discussions. NV would like to thank the Belgian National Fund for Scientific Research for a research grant (FRFC Convention 2.4533.91) and the Communauté Française of Belgium for their financial support provided by the research convention ARC-93/98-166. This work was sponsored by the Stichting Nationale Computerfaciliteiten (National Computing Facilities Foundation, NCF) for the use of supercomputer facilities with financial support from the Nederlandse Organisatie voor Wetenschappelijk Onderzoek (Netherlands Organization for Scientific Research, NWO).

## References

- Bachau H 1984 *J. Phys. B: At. Mol. Phys.* **17** 1771-84  
 —1993 *The Physics of Electronic and Atomic Collisions (Proc. XVIII Int. Conf. Aarhus, 1993)* (AIP Conf. Proc. 295) ed T Andersen *et al* (New York: AIP) pp 547-57  
 Bachau H, Roncin P and Harel C 1992 *J. Phys. B: At. Mol. Opt. Phys.* **25** L109-15  
 Bachau H, Harel C, Barat M, Roncin P, Bordenave-Montesquieu A, Moretto-Capelle P, Benoit-Cattin P, Gleizes A and Benhenni M 1993 *VI Int. Conf. Physics of Highly Charged Ions (Manhattan, Kansas 1992)* (AIP Conf. Proc. 274) ed P Richard *et al* (New York: AIP) pp 175-8  
 Bachau H and Sánchez I 1995 *The Physics of Highly Charged Ions (Proc. VII Int. Conf. Vienna, 1994)* ed F Aumayr, G Betz and H P Winter *Nucl. Instrum. Methods B* **98** 78-80  
 Bárány A, Astner G, Cederquist H, Danared H, Hultdt S, Hvelplund P, Johnson A, Knudsen H, Liljeby L and Rensfelt K-G 1985 *Nucl. Instrum. Methods B* **9** 397  
 Bordenave-Montesquieu A, Benoit-Cattin P, Boudjema M, Gleizes A and Bachau H 1987 *J. Phys. B: At. Mol. Phys.* **20** L695-703  
 Bordenave-Montesquieu A, Moretto-Capelle P, Gonzalez A, Benhenni M, Bachau H and Sánchez I 1994 *J. Phys. B: At. Mol. Opt. Phys.* **27** 4243-61  
 Chen Z and Lin C D 1991 *J. Phys. B: At. Mol. Opt. Phys.* **24** 4231-44  
 Chetoui A *et al* 1990 *J. Phys. B: At. Mol. Opt. Phys.* **23** 3659-75

- Cooke W E and Gallagher T R 1979 *Phys. Rev. A* **19** 2151-3
- Davidson E R 1975 *J. Comput. Phys.* **17** 87-94
- Frémont F, Merabet H, Chesnel J Y, Husson X, Lepoutre A, Lecler D, Rieger G and Stolterfoht N 1994 *Phys. Rev. A* **50** 3117-23
- Gaboriaud M N, Roncin P and Barat M 1993 *J. Phys. B: At. Mol. Opt. Phys.* **26** L303-8
- Ho Y K 1980 *Phys. Lett.* **79A** 44-6
- Kazansky A K 1992 *J. Phys. B: At. Mol. Opt. Phys.* **25** L381-7
- Kazansky A K and Roncin P 1994 *J. Phys. B: At. Mol. Opt. Phys.* **27** 5537-50
- Mack M, Nijland J H, van der Straten P, Niehaus A and Morgenstern R 1989 *Phys. Rev. A* **39** 3846-54
- Martín F, Riera A and Sánchez I 1991 *J. Chem. Phys.* **94** 4275-81
- Martin S, Bernard J, Denis A, Désesquelles J, Chen Li and Ouerdane Y 1994 *Phys. Rev. A* **50** 2322-6
- Merzbacher E 1961 *Quantum Mechanics* (New York: Wiley)
- Niehaus A 1986 *J. Phys. B: At. Mol. Opt. Phys.* **19** 2925-37
- de Nijs G, Hoekstra R and Morgenstern R 1994 *J. Phys. B: At. Mol. Opt. Phys.* **27** 2557-67
- Posthumus J H and Morgenstern R 1990 *J. Phys. B: At. Mol. Opt. Phys.* **23** 2293-304
- Posthumus J H, Lukey P and Morgenstern R 1992 *J. Phys. B: At. Mol. Opt. Phys.* **25** 987-99
- Roncin P 1993 private communication
- Roncin P, Gaboriaud M N and Barat M 1991 *Europhys. Lett.* **16** 551-6
- Roncin P, Gaboriaud M N, Barat M, Bordenave-Montesquieu A, Moretto-Capelle P, Benhenni M, Bachau H and Harel C 1993a *J. Phys. B: At. Mol. Opt. Phys.* **26** 4181-99
- Roncin P, Gaboriaud M N, Szilagyi Z and Barat M 1993b *The Physics of Electronic and Atomic Collisions (Proc. XVIII Int. Conf. Aarhus, 1993)* (AIP Conf. Proc. 295) ed T Andersen et al (New York: AIP) pp 537-46
- Sánchez I and Bachau H 1995 *J. Phys. B: At. Mol. Opt. Phys.* **28** 795-806
- Stolterfoht N 1993 *Phys. Scr.* **T46** 22-33
- Stolterfoht N, Havener C C, Phaneuf R A, Swenson J K, Shafroth S M and Meyer F W 1986 *Phys. Rev. Lett.* **57** 74-7
- Stolterfoht N, Sommer K, Swenson J K, Havener C C and Meyer F W 1990 *Phys. Rev. A* **42** 5396-405
- Vaeck N and Hansen J E 1993 *J. Phys. B: At. Mol. Opt. Phys.* **26** 2977-80
- Vaeck N, van der Hart H W and Hansen J E 1993a *VI Int. Conf. Physics Highly Charged Ions (Manhattan, Kansas 1992)* (AIP Conf. Proc. 274) ed P Richard et al (New York: AIP) pp 414-18
- 1993b *The Physics of Electronic and Atomic Collisions (Proc. XVIII Int. Conf. Aarhus, 1993)* (AIP Conf. Proc. 295) ed T Andersen et al (New York: AIP) pp 794-802
- van der Hart H W and Hansen J E 1993 *J. Phys. B: At. Mol. Opt. Phys.* **26** 641-62
- 1994 *J. Phys. B: At. Mol. Opt. Phys.* **27** L395-400
- van der Hart H W, Vaeck N and Hansen J E 1994 *J. Phys. B: At. Mol. Opt. Phys.* **27** 3489-514
- Wu W, Giese J P, Chen Z, Ali R, Cocke C L, Richard P and Stöckli M 1994 *Phys. Rev. A* **50** 502-10